Phase stability of binary non-additive hard-sphere mixtures. A self-consistent integral equation study. J Chem Phys

ARTICLE *in* THE JOURNAL OF CHEMICAL PHYSICS · MARCH 1996

Impact Factor: 2.95 · DOI: 10.1063/1.471229

4 AUTHORS, INCLUDING:

Enrique Lomba
Institute of Physical Chemistry, CSIC
146 PUBLICATIONS **1,901** CITATIONS
SEE PROFILE

Lloyd L. Lee
California State Polytechnic University, Pom…
139 PUBLICATIONS **2,536** CITATIONS
SEE PROFILE

Noé G. Almarza
Spanish National Research Council
95 PUBLICATIONS **1,071** CITATIONS
SEE PROFILE

Phase stability of binary nonadditive hardsphere mixtures: A selfconsistent integral equation study

E. Lomba, M. Alvarez, L. L. Lee, and N. G. Almarza

Citation: J. Chem. Phys. **104**, 4180 (1996); doi: 10.1063/1.471229
View online: http://dx.doi.org/10.1063/1.471229
View Table of Contents: http://jcp.aip.org/resource/1/JCPSA6/v104/i11
Published by the AIP Publishing LLC.

Phase stability of binary non-additive hard-sphere mixtures: A self-consistent integral equation study

E. Lomba and M. Alvarez
Instituto de Química Física Rocasolano, CSIC, Serrano 119, E-28006 Madrid, Spain

L. L. Lee
School of Chemical Engineering and Materials Science, University of Oklahoma, Norman, Oklahoma 73019

N. G. Almarza
Depto. Química Física I, U. Complutense, E-28040 Madrid, Spain

(Received 7 July 1995; accepted 22 November 1995)

We have tested the capabilities of a new self-consistent integral equation, closely connected with Verlet's modified closure, for the study of fluid-fluid phase separation in symmetric non-additive hard-sphere mixtures. New expressions to evaluate the chemical potential of mixtures are presented and play a key role in the construction of the phase diagram. The new integral equation, which implements consistency between virial and fluctuation theorem routes to the isothermal compressibility, together with chemical potential and virial pressure consistency via the Gibbs-Duhem relation, yields a phase diagram which especially at high densities agrees remarkably well with the new semi-Grand Ensemble Monte Carlo simulation data also presented in this work. Deviations close to the critical point can be understood as a consequence of the inability to enforce virial-fluctuation consistency in the neighborhood of the spinodal decomposition curve. © *1996 American Institute of Physics.* [S0021-9606(96)50309-8]

I. INTRODUCTION

It has been known for years that the microscopic structure of fluids under extremely high pressures is essentially the result of the purely repulsive interactions, i.e. the fluid structure is controlled by excluded volume effects. Therefore, the experimental evidence that certain fluid mixtures undergo fluid-fluid phase separation at very high pressures[1] has induced a renewed interest in one of the simplest theoretical models that can exhibit a similar type of transition (i.e. phase separation induced by excluded volume effects), the Non-Additive Hard Sphere model (NAHS). This model consists of a mixture of hard spheres of diameter $\sigma_{\alpha\alpha}$ (where α denotes the species) whose interactions between unlike particles are characterized by a hard-sphere diameter $\sigma_{\alpha\nu}=1/2(\sigma_{\alpha\alpha}+\sigma_{\nu\nu})(1+\Delta)$, with Δ being the non-additivity parameter. Although there is some evidence that the phase separation might also exhibit in purely additive ($\Delta=0$) but highly asymmetric ($\sigma_{\alpha\alpha}\gg\sigma_{\nu\nu}$) systems[2] due to osmotic depletion effects, the latter situation remains unclear, in particular because of the difficulties associated with the high densities at which the phase transition is expected to occur. In contrast, NAHS systems with positive non-additivity are known to undergo fluid-fluid phase separation easily at moderate densities, and therefore they have been the focus of an important number of recent works in which both simulation techniques[3–5] and integral equation (IE) and perturbation theories[1,6] have been widely explored in an attempt to describe the phase separation phenomenon.

Despite all these efforts, there remains an important gap to be filled concerning the use of integral equation theories in this context. The information extracted from them reduces so far to the localization of the stability boundaries (spinodal curves) and the critical (consolute) point. The limitation stems from the fact that, with the exception of the Hypernetted Chain Equation (HNC),[7] direct and closed expressions to evaluate chemical potentials from the correlation functions were unavailable, and hence a determination of the equilibrium (binodal) curve would require the use of tedious thermodynamic integration procedures,[8] which in the case of mixtures would be extremely cumbersome. Resorting to the HNC theory would be of no avail, given the poor performance of this approximation for purely repulsive potentials. We have here overcome these difficulties resorting to Lee's star function approach[9] in order to derive a direct and closed expression for the evaluation of the chemical potential for mixtures. This expression is presented in this work explicitly for one of the most accurate closures for repulsive systems, Verlet's Modified approximation (VM),[10,11] which we have conveniently rewritten for hard-sphere mixtures. As has been noted by Lomba and Lee,[12,13] this closure is particularly suitable to incorporate thermodynamic consistency conditions without any change in its functional form. Forcing local consistency between virial pressure and isothermal compressibility, together with the virial pressure and chemical potential (via the Gibbs–Duhem thermodynamic relation) defines a Doubly Self-Consistent VM closure, which will be denoted hereafter SC2VM.

Both SC2VM and VM closures have been here investigated in some depth for the simplest NAHS model, namely the binary symmetric NAHS ($\sigma_{11}=\sigma_{22}$), and compared with the results of new semi-Grand Ensemble Monte Carlo (SGMC) simulation data also presented in this work. We will see that the enforcement of thermodynamic consistency improves considerably the results, both for the phase coexistence and thermodynamic properties. Unfortunately, there is

 0021-9606/96/104(11)/4180/9/$10.00

an important region in the neighborhood of the spinodal decomposition curve in which the consistency conditions must be relaxed, i.e. the parametric dependence of the VM bridge function is not flexible enough to account for the changes in the long range behavior of the correlation functions close to the consolute point. Despite this drawback, the SC2VM closure appears as a new promising theoretical tool.

The rest of the paper can be sketched as follows. Essentials of the integral equation theory relevant to this work are summarized in Section II. The derivation of the direct formulas for the evaluation of chemical potentials in mixtures (in particular for VM and SC2VM approximations) is presented is Section III. Details of the semi-Grand Ensemble Monte Carlo simulation techniques employed in this work can be found in Section IV. Finally, the most representative results are presented and analyzed in Section V.

II. SKETCHES OF THE THEORY

The starting point of our treatment is the Ornstein–Zernike (OZ) equation for multicomponent systems, which reads

$$h_{\alpha\nu}(r)=c_{\alpha\nu}(r)+\sum_{l}\rho_l\int d\mathbf{r}'c_{\alpha l}(r')h_{l\nu}(|\mathbf{r}-\mathbf{r}'|) \quad (1)$$

where, $h_{\alpha\nu}(r)=g_{\alpha\nu}(r)-1$ is the total pair correlation function, $g_{\alpha\nu}(r)$ being the pair distribution function, $c_{\alpha\nu}(r)$, the direct correlation function and ρ_l is the number density of species l. Eq. (1) can be written down in a more compact notation by introducing the density-scaled Fourier transforms

$$\tilde{C}_{\alpha\nu}(k)=(\rho_\alpha\rho_\nu)^{1/2}\tilde{c}_{\alpha\nu}(k) \quad (2)$$

and similarly

$$\tilde{H}_{\alpha\nu}(k)=(\rho_\alpha\rho_\nu)^{1/2}\tilde{h}_{\alpha\nu}(k) \quad (3)$$

With this, Eq. (1) in Fourier space becomes,

$$\tilde{\mathbf{H}}(k)=\tilde{\mathbf{C}}(k)[\tilde{\mathbf{I}}-\tilde{\mathbf{C}}(k)]^{-1} \quad (4)$$

where obviously $(\tilde{\mathbf{H}})_{\alpha\nu}=\tilde{H}_{\alpha\nu}(k)$ and $\mathbf{I}$ is the identity matrix.

The OZ equation can be solved when a *closure*, i.e., a relation that connects $h_{\alpha\nu}$ and $c_{\alpha\nu}$, is given. The general closure relation can be formally expressed as follows,

$$g_{\alpha\nu}(r)=\exp[h_{\alpha\nu}(r)-c_{\alpha\nu}(r)-\beta u_{\alpha\nu}(r)+B_{\alpha\nu}(r)] \quad (5)$$

with $\beta=(k_BT)^{-1}$; $u_{\alpha\nu}(r)$ is the interparticle interaction and $B_{\alpha\nu}(r)$ refers to the bridge function, a quantity that is usually unknown. Integral equation techniques will provide the structure of a liquid mixture and its thermodynamic properties if and only if an explicit approximation is given for the bridge function. Unfortunately approximate closures give rise to thermodynamic inconsistencies, which means that different routes to obtain the same quantity lead to different results. A thermodynamic self-consistency criterion can then be assumed as an internal measure of the quality of the closure and this has further been confirmed by comparing self-consistent theories such as the Hybrid Mean Spherical Approximation (HMSA)[14] with simulation data. On the other hand, recently it has been shown that the VM closure yields excellent results for hard-core potentials.[11] This approximation, additionally has a functional form which is easy to parameterize in order to facilitate the introduction of consistency conditions. A straightforward generalization of the VM bridge function for multicomponent systems can be written as

$$B_{\alpha\nu}(r)=-\frac{\Phi_{\alpha\nu}(r;\varphi)\gamma_{\alpha\nu}(r)^2}{2[1+\alpha_{\alpha\nu}\gamma_{\alpha\nu}(r)]} \quad (6)$$

where $\alpha_{\alpha\nu}=\vartheta(1.1-\rho\sigma_{\alpha\nu}^3/3)$ and $\gamma_{\alpha\nu}=h_{\alpha\nu}-c_{\alpha\nu}$ is the indirect correlation function. With $\vartheta=\Phi(r)=1$ we will have the VM closure for mixtures. $\Phi_{\alpha\nu}(r;\varphi)$ may be a simple r-function whose dependence on the parameter φ is to be chosen in a somewhat *ad hoc* fashion. Thus, in Ref. 12 Lomba and Lee used a constant value $\Phi_{\alpha\nu}(r;\varphi)=\varphi$ in their study of monoatomic Lennard-Jones fluids. We have found, however, that to achieve an arbitrary degree of self-consistency, the parametric dependence of $B_{\alpha\nu}(r)$ on φ inside the core must be minimized. After some investigations we found that the function

$$\Phi_{\alpha\nu}(r;\varphi)=1+[1+\tanh(r-\sigma_{\alpha\nu})]\frac{(\varphi-1)}{2} \quad (7)$$

can produce fully self-consistent results (without residual inaccuracies). Unfortunately, the use of this function has a negative effect on the fulfillment of the zero-separation theorem, i.e. the accordance between $B_{\alpha\nu}(0)-C_{\alpha\nu}(0)-1$ and the excess chemical potential calculated from the correlation functions worsens. Despite this drawback the results for the thermodynamic properties evaluated as indicated below can be regarded as excellent.

The double consistency, imposed via the optimization of the two parameters φ and ϑ, is summarized as follows:

(1) One of the consistency criteria relies on the comparison of the isothermal compressibilities, χ_T, calculated both from the fluctuation and the virial theorems. The partial inverse compressibilities (or isothermal bulk modulus, B_T) can be calculated directly from the $k\to 0$ limit of the Fourier transform of the direct correlation function $\tilde{c}_{\alpha\nu}(k=0)$ as follows,

$$\frac{\chi^{id}}{\chi_T}=B_T=\left(\beta\frac{\partial P_c}{\partial\rho}\right)_T=1-\rho\sum_{\alpha,\nu}x_\alpha x_\nu\tilde{c}_{\alpha\nu}(0) \quad (8)$$

where ρ is the total number density and x_ν refers to the mol fraction of species ν. Alternatively, B_T can be determined by numerical differentiation of the virial pressure, P_v, which for hard-sphere mixtures reads,

$$z_v=\frac{\beta P_v}{\rho}=1+2/3\pi\rho\sum_{\alpha,\nu}x_\alpha x_\nu\sigma_{\alpha\nu}^3 g_{\alpha\nu}(\sigma_{\alpha\nu}). \quad (9)$$

Therefore, consistency between the fluctuation-dissipation theorem, Eq. (8), and the virial theorem, Eq. (9), i.e.,

$$\left(\frac{\partial\beta P_c}{\partial\rho}\right)=\left(\frac{\partial\rho z_v}{\partial\rho}\right), \quad (10)$$

is one of the thermodynamic criteria to be required.

(2) On the other hand, with fully consistent thermodynamics, the excess Helmholtz free energy, A^{ex}, should obey the following relation,

$$\rho\left(\frac{\partial \beta A^{\mathrm{ex}}}{\partial \rho}\right)=z_v-1 \tag{11}$$

where z_v is calculated via the virial equation (9), and $\beta A^{\mathrm{ex}}/\rho$ can be determined from the Gibbs free energy through the calculation of the chemical potentials corresponding to each species. Additionally, this relation can be rewritten as the well-known Gibbs–Duhem relation,

$$\frac{1}{\rho}=x_1\left(\frac{d\mu_1}{dP_v}\right)+x_2\left(\frac{d\mu_2}{dP_v}\right) \tag{12}$$

which can be shown to be identical to Eq. (11).

The determination of A^{ex} or ρ via the chemical potential route has been made feasible due to the introduction of closed, direct expressions for the calculation of μ_α in terms of correlation functions, which will be derived in the next section.

Since the integral equation approach used can only be applied to homogeneous fluids, our analysis of the thermodynamic stability and phase equilibria will be restricted to an attempt to determine the absolute limits of material stability for one-phase NAHS mixture, i.e., the spinodal curve, and the phase coexistence, that is to say the binodal curve. The latter will be obtained by applying equilibrium conditions to the integral equation thermodynamic results. In principle, a spinodal curve could be derived from thermodynamics (locating the thermodynamic states that fulfill $(\partial\mu_\nu/\partial x_\nu)=0$), but is clearly more interesting to use structural information to locate the boundary. This is done by characterizing the divergence of the long-wavelength limit of the concentration-concentration Bathia-Thornton structure factor $S_{\mathrm{cc}}(k=0)$.[15] After solving the OZ equations, $S_{\mathrm{cc}}(0)$ can be evaluated from,

$$\frac{S_{\mathrm{cc}}^{(M)}(0)}{\Pi_M x_m}=\frac{1}{(\rho k_B T\chi_T)|\mathbf{I}-\tilde{\mathbf{C}}(0)|}=\frac{B_T}{|\mathbf{I}-\tilde{\mathbf{C}}(0)|}=\frac{B_T}{D(0)} \tag{13}$$

which is a general expression for M-component mixtures.[16] At the demixing spinodal, B_T usually remains positive and finite while $D(0)$ vanishes. $S_{\mathrm{cc}}(0)$ can be understood as the global measure of deviations from the mean concentration. The discrepancies between the ''thermodynamic'' spinodal and its structural counterpart will be an assessment of the thermodynamic inconsistency of the approximation being used. Finally, notice that, by definition the increasingly long range of the concentration correlations as the divergence is approached, implies the break down of the numerical solution of the OZ equation via Eq. (4).

III. DIRECT CHEMICAL POTENTIAL FORMULAS IN A MIXTURE

The derivation of a closed form for the chemical potentials of a fluid mixture that involves only integrals of correlation distribution functions at the given state, is presented in what follows.

For a mixture of two species, 1 and 2, with N_1 and N_2 being the numbers of particles, respectively ($N=N_1+N_2$), the grand canonical partition function is,

$$\Xi=\sum_{N\geqslant 0}\frac{z_1^{N_1}z_2^{N_2}}{N_1!N_2!}\int d\{N\}\exp[-\beta V_N-\beta W_N] \tag{14}$$

where V_N is the sum of pair interactions $u_{\alpha\nu}$, and W_N, the sum of external forces due to the two test particles of species 1 and 2 at positions $\mathbf{t}_1$ and $\mathbf{t}_2$, respectively. (Note the one can turn on test particle 1 or 2, alternatively)

$$V_N(\{N\})\equiv\sum_i\sum_{j>1}^{N}u_{\alpha\nu}(r_{ij})=\sum_i\sum_{j>1}^{N}u_{\alpha\nu}(i,j);\quad \alpha,\nu=1,2, \tag{15}$$

$$W_N(\{N\})\equiv\sum_i^N u_{\alpha a}(i,t_1)+\sum_j^N u_{\nu b}(j,t_2). \tag{16}$$

Using the partition function variational method of Lee,[9] we have the following equality,

$$\frac{\partial \ln\Xi[0]}{\partial z_1}=N_1\Lambda_1^3\exp(-\beta\mu_1)=\int d\mathbf{t}_1\frac{\Xi[w_1]}{\Xi[0]}. \tag{17}$$

When we expand in Taylor series the partition function as $\exp(\ln\Xi[w_1]-\ln\Xi[0])$, we obtain after some algebra, the excess chemical potential (over the ideal gas value) of species 1,

$$\beta\mu_1^{\mathrm{ex}}=\sum_\nu\rho_\nu\int d\mathbf{r}\Big[\gamma_{1\nu}+B_{1\nu}-h_{1\nu}+\frac{1}{2}h_{1\nu}\gamma_{1\nu}+h_{1\nu}B_{1\nu}-S_{1\nu}\Big] \tag{18}$$

(with a similar formula for species 2), where $S_{1\nu}$ is the star function introduced earlier by Lee[17] (under the *unique function* assumption, see Ref. 17)

$$S_{1\nu}(r)\approx\frac{h_{1\nu}(r)}{\gamma_{1\nu}(r)}\int_0^{\gamma_{1\nu}}d\gamma'_{1\nu}B_{1\nu}(\gamma'_{1\nu};r). \tag{19}$$

When a particular closure is used for $B_{1\nu}$, Eq. (19) can be evaluated by integrating with respect to the indirect correlation functions $\gamma_{1\nu}$. Particularly, when Eq. (6) is the closure, the integration can be explicitly performed to yield,

$$\int_0^{\gamma_{1\nu}}d\gamma'_{1\nu}B_{1\nu}(\gamma'_{1\nu})=-\frac{\Phi_{1\nu}}{4\alpha_{1\nu}^3}[(1+\alpha_{1\nu}\gamma_{1\nu})^2-4(1+\alpha_{1\nu}\gamma_{1\nu})+2\ln(1+\alpha_{1\nu}\gamma_{1\nu})+3]. \tag{20}$$

Equations (18)–(20) give the desired result for the excess chemical potential.

IV. SEMI-GRAND ENSEMBLE MONTE CARLO SIMULATIONS

Amar[4] performed simulations for the NAHS model using the Gibbs-Ensemble Monte Carlo method.[18–20] However, one can take full advantage of the symmetry properties of this system and carry out simulations in the so-called semi-Grand Ensemble,[21,22] which turns out to be considerably simpler, as will be shown below.

The change in Gibbs free energy in a symmetric NAHS mixture can be written as

$$d(\beta G)=Ud\beta+Vd(\beta P)+\beta\mu_1 dN_1+\beta\mu_2 dN_2. \tag{21}$$

This equation transforms into

$$d(\beta G)=Ud\beta+Vd(\beta P)+\beta\mu_1 dN+\beta\Delta\mu dN_2 \tag{22}$$

where $N=N_1+N_2$ and $\Delta\mu=\mu_2-\mu_1$, which after some rearrangement leads to

$$d(\beta G-\beta N_2\Delta\mu)=Ud\beta+Vd(\beta P)+\beta\mu_1 dN - N_2 d(\beta\Delta\mu). \tag{23}$$

If we have two phases with different compositions (I and II), the symmetry of the interactions imposes the equilibrium relation

$$x_1^{\mathrm{I}}=x_2^{\mathrm{II}} \tag{24}$$

and therefore

$$\mu_1^{\mathrm{I}}=\mu_1^{\mathrm{II}}=\mu_2^{\mathrm{I}}=\mu_2^{\mathrm{II}} \tag{25}$$

that is, at equilibrium, $\Delta\mu=0$.

The partition function of the system (Eq. (14) can also be written as [22]

$$\Xi=\frac{1}{\Lambda^{3N}}\sum_{N_1=0}^{N}\frac{N!}{N_1!(N-N_1)!}\times\int dV e^{-\beta PV}V^N\int d\xi_1^{N_1}\int d\xi_2^{N-N_1}\times\exp(-\beta U(\xi_1^{N_1},\xi_2^{N-N_1},V)) \tag{26}$$

where $\xi_k^{N_k}$ represents the set of coordinates of particles of type k in reduced units (scaled with the length of the simulation box, L). In this equation one considers explicitly the different number of particles of each type. In order to understand the simulation method used herein, it is more convenient to regard the system from a different standpoint. Instead of considering a mixture of N_1+N_2 particles we can view the system as composed of N particles where each can adopt two different identities. Or alternatively each particle is endowed with an additional two-valued internal degree of freedom.

Let ξ^{3N} be the set of box-length reduced position coordinates of the particles. A given configuration will be made explicit by ξ^{3N}, the set of discrete *internal* coordinates I^N (which define the identity of every particle) and the volume V. The partition function can then be written now as

$$\Xi=\frac{1}{\Lambda^{3N}}\int dV\int d\xi^{3N}\sum_{I^N}V^N\exp[-\beta U(\xi^{3N},I^N,V) - \beta PV]. \tag{27}$$

A. Implementation Details

In this representation of the partition function, volume, position coordinates and *identity coordinates* will have to be sampled. In the case of the position coordinates, this has been done following the standard procedure.[23]

For purely hard-core systems, given a set of coordinates ξ^{3N} and I^N, the volume of the system will be distributed with a probability, Π, defined by

$$\Pi(V|\xi^{3N},I^N)=\frac{V^N e^{-\beta PV}}{\int_{V_{\min}}^{\infty}V^N e^{-\beta PV}dV}\quad\text{if}\quad V\geqslant V_{\min}(\xi^{3N},I^N), \tag{28}$$

$$\Pi(V|\xi^{3N},I^N)=0\quad\text{if}\quad V<V_{\min}(\xi^{3N},I^N). \tag{29}$$

Above, $V_{min}(\xi^{3N},I^N)$ is the minimum volume the system can adopt for given values of ξ^{3N} and I^N without causing hard-sphere overlappings. One can then perform volume sampling by generating new values of the volume with probabilities given by $\Pi(V|\xi^{3N},I^N)$. In order to do this one can define $V_M(\xi^{3N},I^N)$, as the volume which maximizes the function $V^N\exp[-\beta U(\xi^{3N},I^N,V)+PV]$, and its value will be

$$V_M(\xi^{3N},I^N)=\max[V_{\min}(\xi^{3N},I^N),N\beta P]. \tag{30}$$

Finally, it is possible to remove the infinite limit in the sampling of volumes with negligible effects on the simulation results by fixing an upper limit value, $V_{\max}(\xi^{3N},I^N)$ so that the value of

$$\epsilon=\frac{\int_{V_{\max}}^{\infty}dVV^N e^{-\beta PV}}{\int_{V_{\min}}^{\infty}dVV^N e^{-\beta PV}} \tag{31}$$

becomes negligible. Since the maximum value of $\Pi(V|\xi^{3N},I^N)$ can be calculated, it is quite simple[24] to design an algorithm that generates values of V according to the probability distribution given by Eq. (28). The algorithm we have used here can be sketched as follows:

(1) Choose a test volume at random, V^{test}, with uniform probability in the range $[V_{\min},V_{\max}]$.

(2) Evaluate $\alpha(V^{\mathrm{test}})=\pi(V^{\mathrm{test}})/\pi(V_M)$, according to Eq. (28).

(3) Generate a random number, η with uniform probability in the interval [0,1]. If $\alpha(V^{\mathrm{test}})\geqslant\eta$, the new volume of the system will be V^{test}. Otherwise go to step (1).

Identity moves are in fact the simplest in the scheme. A particle is chosen at random and the trial configuration is reached by *flipping* its identity, if this change leads to an overlap the identity move is rejected.

We have carried out simulations following the method explained above at several values of βP. In order to check finite size effects we have simulated systems with 500 and

TABLE I. Coexistence data from Monte Carlo simulation.

$\beta P\sigma^3$	N	$\langle\rho\sigma^3\rangle$	x_1	N	$\langle\rho\sigma^3\rangle$	x_1
1.475	1000	0.429(2)	0.335(20)			
1.500	1000	0.438(2)	0.259(38)	500	0.446(5)	0.208(30)
1.525	1000	0.442(2)	0.230(21)			
1.550	1000	0.450(4)	0.185(22)	500	0.456(5)	0.159(27)
1.575	1000	0.455(4)	0.163(16)			
1.600	1000	0.464(3)	0.129(10)	500	0.463(2)	0.128(6)
1.650	1000	0.475(3)	0.101(5)			
1.700	1000	0.483(2)	0.085(3)	500	0.478(2)	0.093(4)
1.750	1000	0.492(3)	0.071(4)			
1.800	1000	0.497(3)	0.064(4)	500	0.495(4)	0.066(5)
1.850	1000	0.508(3)	0.051(3)			
1.900	1000	0.514(2)	0.046(2)	500	0.517(2)	0.044(2)
1.950	1000	0.522(6)	0.039(4)			
2.000	1000	0.530(2)	0.034(2)	500	0.529(3)	0.034(3)
2.050	1000	0.539(2)	0.028(1)			
2.100	1000	0.543(2)	0.025(1)	500	0.543(3)	0.025(2)
2.200	1000	0.554(2)	0.021(1)	500	0.556(5)	0.020(2)
2.300	1000	0.566(2)	0.016(1)	500	0.567(2)	0.016(1)
2.400	1000	0.577(3)	0.013(1)	500	0.578(5)	0.013(1)
2.500	1000	0.590(3)	0.010(1)	500	0.599(3)	0.008(1)

1000 particles. Initial configurations with equal composition were created by generating positions at random in the cubic cell. The initial volume of the system was fixed so that there were no overlapping configurations.

The maximum displacement parameter was chosen to be $0.030L$ and $0.025L$ for simulation with 500 and 1000 particles respectively. The fraction of accepted movements was around 30%. Simulations were arranged in MC-sweeps, in every sweep we first try to translate every particle, we then attempt N identity changes (in this case the spheres are chosen at random) and last we generate a new volume. In all the cases we used 10^5 sweeps to equilibrate the system and subsequent 2×10^5 sweeps were used in the production run. In the averaging procedure values of the properties at the end of each sweep were involved. These values were grouped to calculate averages over blocks of 10^3 sweeps. The analysis of those sub-averages was performed to calculate mean values of properties (volume and composition) and estimate error bars. The calculation of the *correlation length* of the block-averaged values made possible the evaluation of the number of *effectively independent* blocks[23,25] and therefore to calculate a reliable value for the standard deviation of the mean; error bars were set to twice this quantity.

The composition of phases is calculated by using

$$\langle x\rangle = \frac{\langle \min[N_1, N_2]\rangle}{N}. \tag{32}$$

In some applications[26] it seems more accurate to consider x as the compositions (densities in the case of liquid-vapor one component phase equilibria) corresponding to the maxima in the probability distribution histograms rather than averages like that in Eq. (32). Nonetheless, we have found no evidence of strong system size dependence in the results obtained herein using the simpler averaging procedure, which validates our choice. Main simulation results are collected in Table I.

B. Estimation of critical parameters

In order to estimate critical parameters we fitted the simulation results for runs using 1000 particle samples, with $\beta P\sigma^3 \leqslant 1.70$ to the corresponding scaling laws with nonclassical exponents.[19,27] For higher values of $\beta P\sigma^3$ departures from the scaling laws were observed. Our estimates locate the critical point at $\rho_c\sigma^3 = 0.425 \pm 0.005$ $(x_1 = x_2 = 0.5)$ and $\beta P_c\sigma^3 = 1.46 \pm 0.02$.

C. NPT Monte Carlo simulations

In addition to the SGMC simulations we have performed NPT simulations of NAHS mixtures at fixed compositions. This second set of runs were used to cross check the accuracy of SGMC results and also to evaluate chemical potentials by using *particle-insertion* methods. Mol fractions were chosen to be $x = 0.50$ for $\beta P\sigma^3 < \beta P_c\sigma^3$ or those resulting from SGMC simulations for $\beta P\sigma^3 > \beta P_c\sigma^3$. The simulation method is equivalent to that used in SGMC Runs but without performing *identity* moves. Results are summarized in Table II. Consistency between SGMC and NPT results is observed, in the equality (within statistical accuracy) of densities of *equivalent* points in both ensembles and also in the equality of chemical potential of the two species in the NPT results for higher pressures.

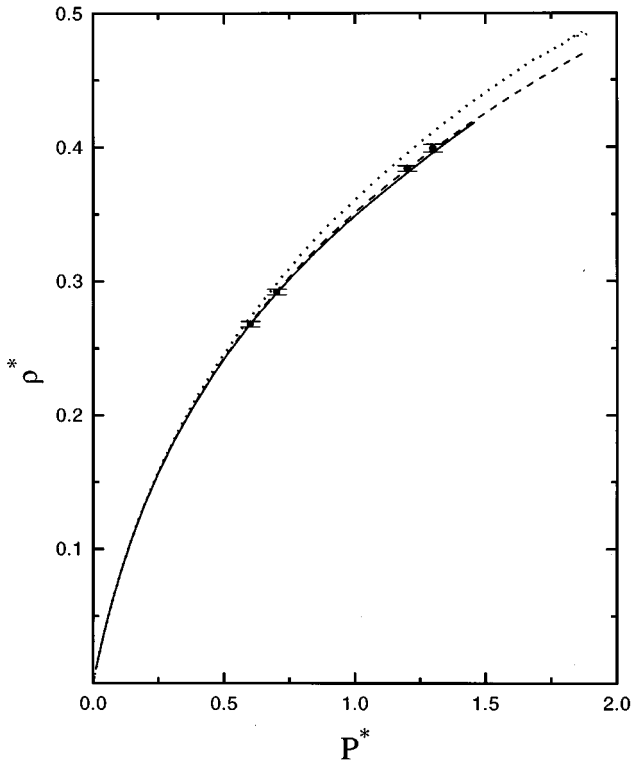

FIG. 1. Pressure dependence of the total density. NPT simulation data (solid circles), SC2VM (continuous line) and VM results (dashed line). The dotted line is the result of applying Gibbs–Duhem equation (12) to the VM chemical potential and virial pressure.

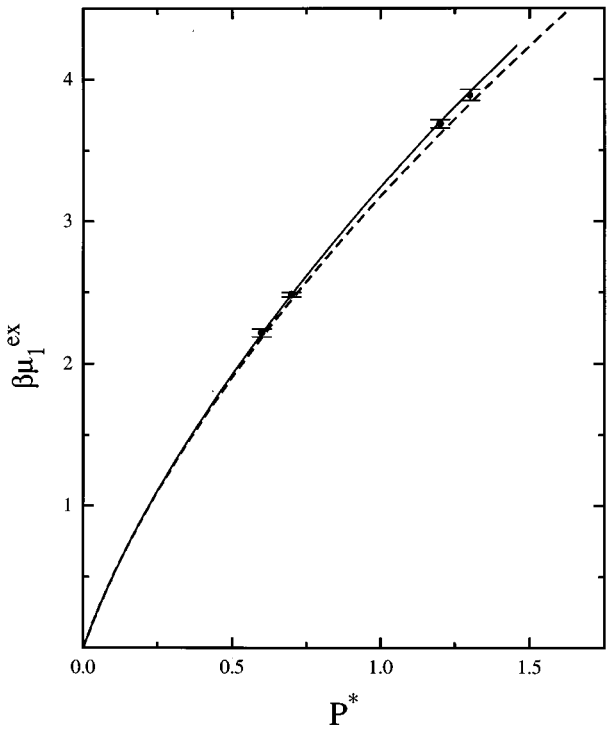

FIG. 2. Pressure dependence of the excess chemical potential. NPT simulation data (solid circles), SC2VM (continuous line) and VM results (dashed line).

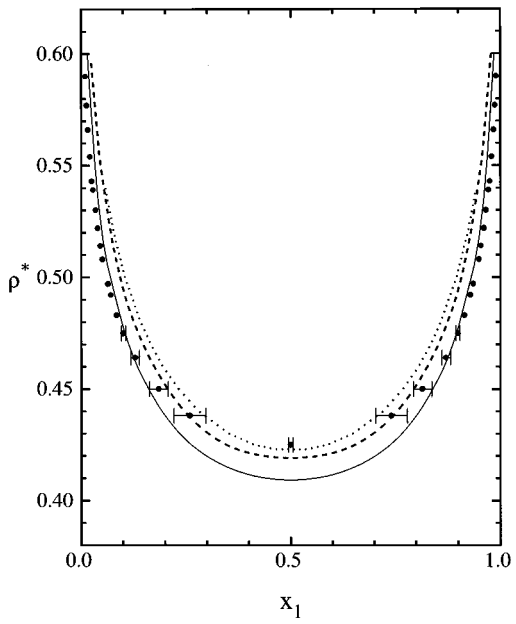

FIG. 3. Coexistence curves for a binary NAHS fluid mixture. SC2VM (continuous line), VM (dashed line), and MIX1 (dotted line) results vs simulation data (solid circles).

V. RESULTS

We have solved both the SC2VM and VM approximations for a model of two-component equal sized hard sphere mixture, $\sigma_{11}=\sigma_{22}=\sigma$. Obviously, explicit attractive interactions are completely neglected though an effective attraction between like particles comes into play, as a result of the positive non-additivity. The non-additive parameter is set to 0.2 which amounts to a cross-interaction hard-sphere diameter $\sigma_{12}=1.2\sigma$. The quality of the integral equations herein considered has been assessed by comparison with NPT simulation data, both for pressures and chemical potentials. In Fig. 1 we have plotted ρ^* *vs* P^* ($\rho^*=\rho\sigma^3$ and $P^*=\beta P\sigma^3$), a natural representation for NPT data, together with the results of the SC2VM and VM approximations for an equimolar mixture. For the latter we have also plotted the value of ρ^* which is obtained when applying the Gibbs–Duhem relation to virial pressure, P_v, and chemical potential, Eq. (12), and one readily appreciates the increasing thermodynamic inconsistency of the VM approximation at high densities. Obviously, Gibbs–Duhem relation applied to SC2VM results yields by construction the same value of density that was used as input for the integral equation calculations. The improvement of the SC2VM over the already good VM results is clear, in particular as far as the chemical potential is concerned (see Fig. 2). We can now proceed to the determination of the phase diagram.

The phase behavior is described by characterizing the coexistence curve (i.e. ρ^*-x_1 diagram) with data obtained from both integral equation approaches. The coexistence curve is defined by the locus of (ρ^*,x_1)-points that fulfill the equilibrium conditions between phases I and II,

$$\mu_\nu^{\mathrm{I}}(x_\nu^{\mathrm{I}},\rho)=\mu_\nu^{\mathrm{II}}(x_\nu^{\mathrm{II}},\rho) \tag{33}$$

$$P^{\mathrm{I}}(x_\nu^{\mathrm{I}},\rho)=P^{\mathrm{II}}(x_\nu^{\mathrm{II}},\rho);(\nu=1,2). \tag{34}$$

The pressure equality forces a particularly simple symmetry condition in our mixture model, in which the role played by species 1 and 2 is completely interchangeable. As has been shown in the previous section, phase equilibrium will be simply defined by the one-phase equation,

$$\mu_1^{\mathrm{I}}(x_1,\rho)=\mu_2^{\mathrm{I}}(x_1,\rho) \tag{35}$$

and

$$x_1^{\mathrm{II}}=1-x_1^{\mathrm{I}}. \tag{36}$$

The SC2VM and VM coexistence curves are plotted in Fig. 3 together with results of the MIX1 theory (a first-order perturbation theory[3]), which is supposed to be fairly accurate for binary NAHS mixtures.[6] It can be seen that the SC2VM theory agrees remarkably well with the simulation data from moderate to high densities out-performing both VM and MIX1 approaches. As the critical density is approached, ''experimental'' data seem to lie closer to the VM and MIX1 curves. It has to be mentioned that the larger discrepancies of the SC2VM theory in the neighborhood of the critical density are due to the fact that the virial-fluctuation theorem self-consistency condition has to be relaxed when approaching the spinodal. This unfortunate situation is known to be common to other self-consistent approximations, like the HMSA, for which the optimization fails to converge for cer-

TABLE II. Chemical potential results from NPT Monte Carlo simulations.

$\beta P\sigma^3$	N	x_2	$\langle\rho\sigma^3\rangle$	$\beta\mu_1$	$\beta\mu_2$
0.60	500	0.500	0.268(2)	0.21(3)	0.21(3)
0.70	500	0.500	0.292(2)	0.56(2)	0.56(2)
1.20	500	0.500	0.384(2)	2.04(4)	2.04(4)
1.30	500	0.500	0.399(3)	2.29(3)	2.29(2)
1.50	1000	0.259	0.437(2)	2.78(2)	2.78(2)
2.00	1000	0.034	0.529(2)	3.79(3)	3.79(4)
2.50	1000	0.010	0.587(3)	4.67(4)	4.61(9)

tain thermodynamic states.[28] Figure 4 depicts the boundary of the zone where double self-consistency could be achieved, together with the coexistence curve. Inside the boundary the virial isothermal compressibility consistency constraint was relaxed, and in the immediate vicinity of the non-solution curve (boundary of the region where convergence could not be achieve by any means) the pressure-chemical potential constraint was set free as well. The largest inconsistency between virial and isothermal compressibility ($\approx$15%) occurs in the vicinity of the critical point. At higher densities the inconsistency varies from 0.5% to 1%.

The $\rho^* - P^*$ and $\beta\mu_1 - P^*$ plots along the coexistence curve are presented both for SC2VM, VM and simulation results in Figs. 5 and 6, respectively. Again, the improvement of the self-consistent approximation is evident. The discrepancies in pressure are however somewhat larger than those obtained for the equimolar mixture (Fig. 1). This might be the result of the uncertainty in the determination of the equilibrium compositions, which magnifies the departures in the pressure calculations at high densities. As to the chemical potentials the SC2VM results can be deemed excellent (Fig. 6).

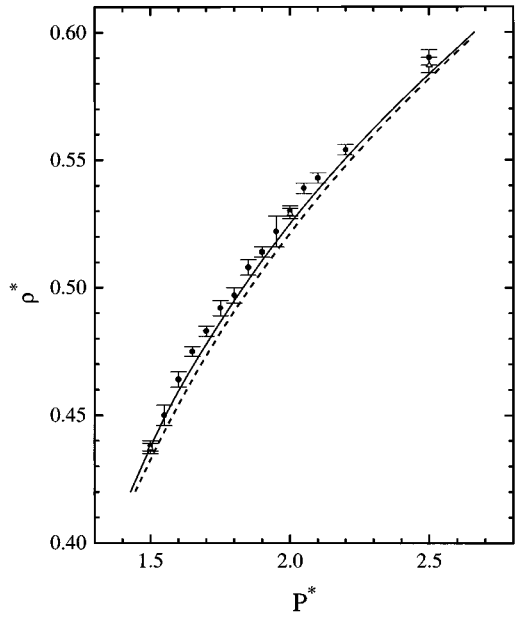

FIG. 5. Pressure dependence of the density along the coexistence curve. SGMC simulation (solid circles) and NPT simulation data (open triangles) together with SC2VM (continuous line) and VM results (dashed line).

As mentioned before, the instability boundary is defined by the divergence of the $S_{cc}(0)$, that is determined by the zeros of $D(0)$ in Eq. (13). Note that instabilities might also occur for finite k, but this would be associated with the ap-

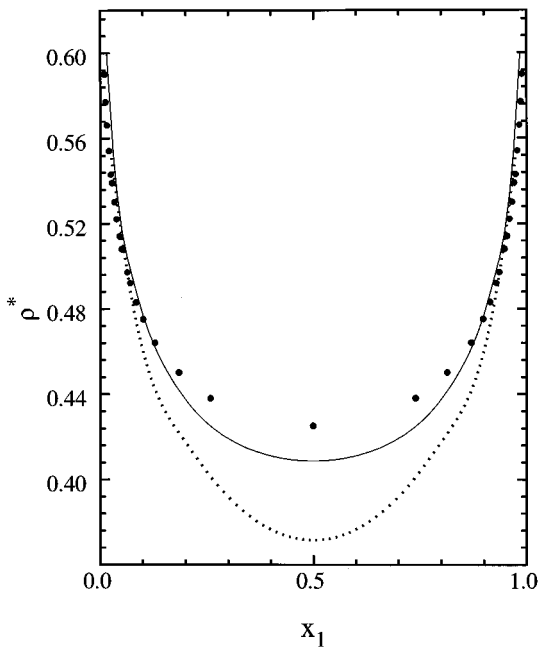

FIG. 4. Double consistency boundary (dotted line), SC2VM coexistence curve (continuous line) and simulation data (solid circles).

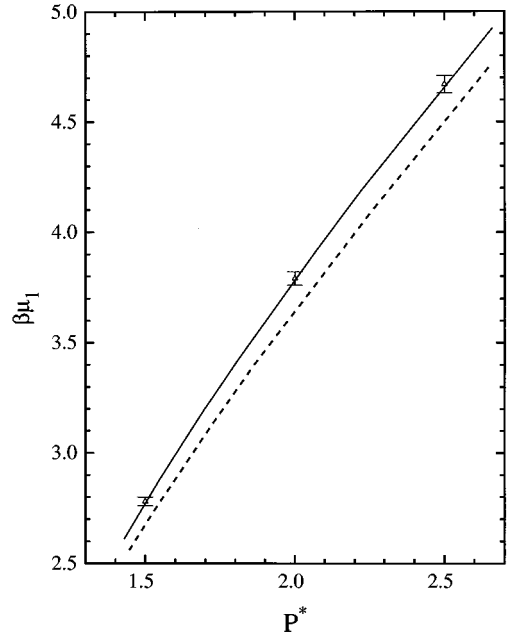

FIG. 6. Pressure dependence of the full chemical potential along the coexistence curve. NPT simulation data (open triangles), SC2VM (continuous line), and VM results (dashed line).

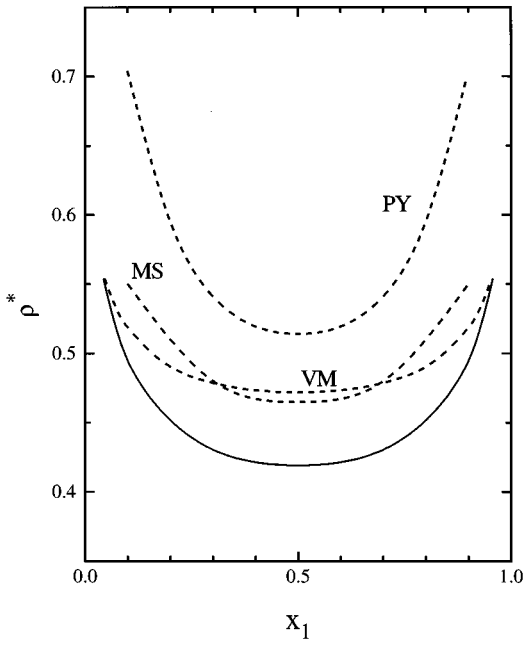

FIG. 7. Spinodal boundaries for different integral equations (VM, PY, and MS) for a binary NAHS mixture. The equilibrium curve corresponding to VM calculations (continuous line) is plotted as a reference.

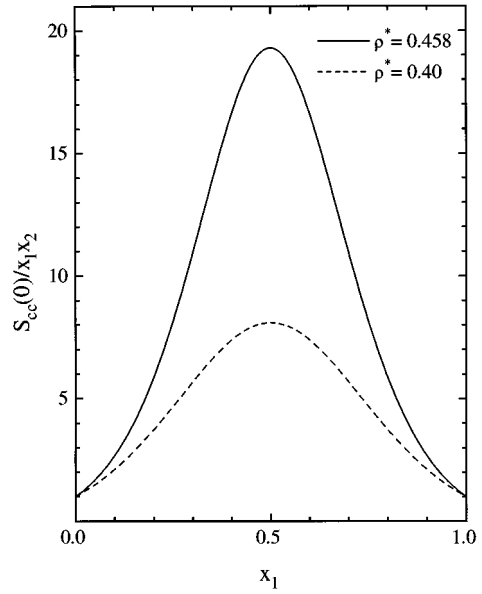

FIG. 9. Density dependence of $S_{cc}(0)/x_1x_2$ close to the consolute point.

pearance of spatially ordered structures, such as lamellar phases, and not with a simple demixing transition. In particular, for a binary mixture $D(k)$ is nothing but

$$D(k)=[1-\rho_1\tilde{c}_{11}(k)][1-\rho_2\tilde{c}_{22}(k)]-\rho_1\rho_2\tilde{c}_{12}^2(k). \tag{37}$$

In Fig. 7 we have plotted estimates of spinodal curves for different IE approximations (Percus-Yevik (PY),[29] Martynov-Sarkisov (MS)[30]) together with our calculations for the VM closure. The solid line refers to the VM equilibrium curve and is displayed in the same figure as a reference. The corresponding non-solution curve for the SC2VM is not plotted, since the relaxation to the consistency conditions from given thermodynamic states does not allow to define a true non-solution pseudo-spinodal curve for the SC2VM theory. In our VM calculations, $D(0)$ never did vanish in the strictest sense although we found it is steeply decreasing when approaching the transition, as can be seen in Fig. 8 for the equimolar mixture. Strictly speaking this means that the spinodal curve is never reached, only a non-solution curve, that might be understood as a signature of an instability boundary. The usual extrapolation procedure to find the values where $1/S_{cc}(0)\rightarrow 0$, is not always legitimate, since a steep fall in the susceptibility can also signal the boundary of complex solutions which is different from the spinodal.[31] As can be noticed in Fig. 8, $D(0)$ is monotonously decreasing with density for $\rho^*>0.25$ in the case of VM calculations, but the SC2VM $D(0)$ shows two singular points (with a discontinuous change in the slope) which are introduced by the relaxation of the two consistency conditions, one at about $\rho^*\approx 0.37$ and the second at $\rho^*\approx 0.41$.

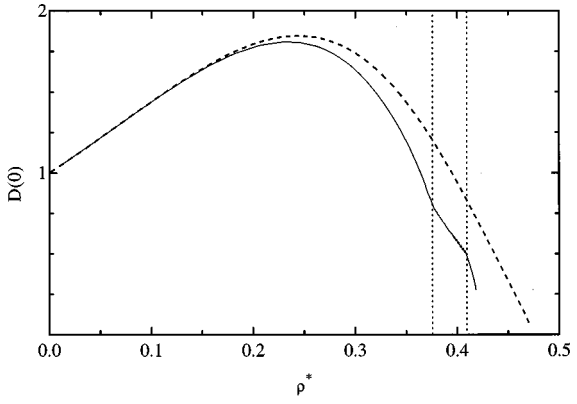

FIG. 8. Density dependence of $D(0)$ for both SC2VM (continuous line) and VM (dashed line) approaches in the case of a equimolar NAHS mixture.

The incipient phase transition can then be located by finding the locus at which the divergence of $S_{cc}(0)$ takes place. This is illustrated in Fig. 9 where the variation of the profile of $S_{cc}(0)/x_1x_2$ *vs* x_1 with increasing total density is shown. The curve is symmetric around the critical mol fraction $x_1=0.5$ as should be expected. Now when comparing Figs. 3 and 7 for the VM approximation, one finds striking evidence of the thermodynamic inconsistency of this closure. The critical (or ''pseudocritical,'' since $D(0)$ does not vanish completely) point obtained from the divergence of $S_{cc}(0)$, is located around $\rho_c^*\approx 0.48$ whereas the critical point derived from thermodynamic data is located at $\rho_c^*\approx 0.42$. Forcing thermodynamic consistency (with the aforementioned limitations) brings the critical density from $D(0)$ (extrapolated from Fig. 8) down to $\rho_c^*\approx 0.43$ which is much closer to the estimate from SC2VM thermodynamics ($\rho_c^*\approx 0.41$). The inconsistency in the VM approach defines a region between the two estimates of the critical density where one can perform calculations over the whole composition range along an iso-

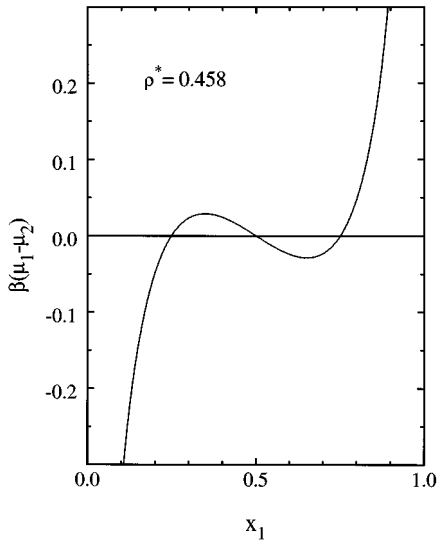

FIG. 10. Variation of $\beta(\mu_1-\mu_2)$ with composition along a subcritical (according to the location of the critical density predicted from thermodynamics) isochore.

chore, and still a demixing transition can be characterized by the behavior of thermodynamic quantities. The quantity of interest is then the difference in chemical potentials, $\beta(\mu_1-\mu_2)$, which has been plotted in Fig. 10. We see that this quantity exhibits a characteristic van der Waals loop, symmetric around $x_1=0.5$, by which obviously a Maxwell equal-area construction would yield the equilibrium condition, $\beta(\mu_1-\mu_2)=0$, i.e., Eq. (35).

In summary, we have here presented an useful application of a new self-consistent integral equation theory to the determination of the coexistence curve in binary mixtures, which rests upon the use of a new closed, direct and single-state formula for the calculation of the chemical potentials. Despite the remarkable agreement between theory and simulation, there is room for further improvement, in particular in the design of more flexible closures that might enable the use of self-consistency conditions in the vicinity of the instability boundaries, i.e. when the correlation functions become long-ranged.

ACKNOWLEDGMENTS

This research was financially supported by the Spanish Dirección General de Investigación Cientí fica y Técnica (DGICYT) under Grants No. PB94-0112 and PB92-0114-C04.

[1] J. Jung, M. S. Jhon, and F. H. Ree, J. Chem. Phys. **102**, 1349 (1995).
[2] T. Biben and J.-P. Hansen, Phys. Rev. Lett. **66**, 2215 (1991).
[3] T. W. Melnyk and B. L. Sawford, Mol. Phys. **29**, 891 (1975).
[4] J. G. Amar, Mol. Phys. **67**, 739 (1989).
[5] M. Schoen and C. Hoheisel, Mol. Phys. **53**, 1367; *ibid.* **57**, 65 (1986).
[6] D. Gazillo, J. Chem. Phys. **95**, 4565 (1991); Mol. Phys. **84**, 303 (1995).
[7] T. Morita and K. Hiroike, Prog. Theor. Phys. **23**, 1003 (1960).
[8] See C. Caccamo, P. V. Giaquinta, and G. Giunta, J. Phys. Cond. Matter **B 75**, 5 (1993), for an application of thermodynamic integration to the determination of the gas-liquid equilibrium Lennard-Jones fluids in the HMSA.
[9] L. L. Lee, J. Chem. Phys. **97**, 8606 (1992).
[10] L. Verlet, Mol. Phys. **41**, 183 (1980).
[11] S. Labik, A. Malijevsky, and W. R. Smith, Mol. Phys. **73**, 87 (1991).
[12] E. Lomba and L. L. Lee, Int. J. Thermophys. **17**, 663 (1996).
[13] L. L. Lee, D. Ghonasgi, and E. Lomba (to be published) .
[14] G. Zerah and J. P. Hansen, J. Chem. Phys. **84**, 2336 (1986).
[15] A. B. Bathia and D. E. Thornton, Phys. Rev. B **2**, 3004 (1970).
[16] D. Gazillo, Mol. Phys. **83**, 1171 (1994).
[17] L. L. Lee, J. Chem. Phys., **60**, 1197 (1974).
[18] A. Z. Pangiotopoulos, Mol. Sim. **9**, 1 (1992).
[19] B. Smit, in *Computer Simulation in Chemical Physics*, edited by M. P. Allen and D. J. Tildesley (Kluwer, Dordrecht, 1993).
[20] A. Z. Pangiotopoulos, in *Observation, Prediction and Simulation of Phase Transitions in Complex Fluids*, edited by M. Baus, L. F. Rull, and J.P. Ryckaert (Kluwer, Dordrecht, 1995).
[21] D. A. Kofke and E. D. Glandt, Mol. Phys. **64**, 1105 (1988).
[22] D. Frenkel, in *Computer Simulation in Chemical Physics*, edited by M. P. Allen and D. J. Tildesley (Kluwer, Dordrecht, 1993).
[23] M. P. Allen and D. J. Tildesley, *Computer Simulation of Liquids* (Clarendon, Oxford, 1987).
[24] W. H. Press, B. P. Flannery, S. A. Teukolsky, and W. T. Vetterling, *Numerical Recipes, The Art of Scientific Computing* (Cambridge University, Cambridge, 1988).
[25] M. P. Allen, in *Computer Simulation in Chemical Physics*, edited by M. P. Allen and D. J. Tildesley (Kluwer, Dordrecht, 1993).
[26] J. R. Recht and A. Z. Pangiotopoulos, Mol. Phys. **80**, 843 (1993).
[27] J. S. Rowlinson and F. L. Swinton, *Liquid and Liquid Mixtures*, 3rd ed. (Butterworths, London, 1982).
[28] P. Salgi, J.-F. Guérin, and R. Rajagopalan, Coll. Polym. Sci. **270**, 785 (1992).
[29] J. P. Hansen and I. R. McDonald, *Theory of Simple Liquids* (Academic, London, 1986).
[30] G. A. Martynov and G. N. Sarkisov, Mol. Phys. **49**, 1495 (1983).
[31] J. S. Høye, E. Lomba, and G. Stell, Mol. Phys. **79**, 523 (1993); E. Lomba and J. L. López-Martín, J. Stat. Phys. **80**, 825 (1995).